JSAP Review
JSAP Rev. **2025**, 250206
https://doi.org/10.11470/jsaprev.250206

Tutorial Review

The first formation of ion tracks in diamond via MeV C_{60} ion irradiation

Hiroshi Amekura

National Institute for Materials Science (NIMS), Tsukuba, Ibaraki 305-0003, Japan
E-mail: amekura.hiroshi@nims.go.jp

Injecting high-energy heavy ions into solids can create cylindrical damage zones called ion tracks. The most accepted mechanism for ion track formation is the inelastic thermal spike (i-TS) model in which molten regions induced by large energy deposition along the ion trajectories transform to tracks after quenching. However, diamond, which is in a meta-stable state, does not melt with heating but transforms to a stable state (i.e., graphite). While no tracks have ever been observed in diamond, we successfully formed tracks under MeV C_{60} ion irradiation. Track formation via a non-melting route is presented herein.

Received December 23, 2024; Accepted January 27, 2025
Translated from Oyo Buturi **94**, 237 (2025) DOI: https://doi.org/10.11470/oubutsu.94.5_237

1. Introduction

Ion beams are crucial for fabricating semiconductor integrated devices, and the interactions between monatomic ions and materials in the energy range from sub-keV to several MeV have already been thoroughly studied owing to their industrial importance. The "ion tracks," the focus of this review, were previously considered to form only at higher energies, typically exceeding 10 MeV. However, recent research has shown that ion tracks can also be formed at lower energies, on the order of several MeV, when cluster ions such as C_{60} are used. This review sought to introduce the physics underlying the phenomenon wherein cluster ions can form tracks more efficiently at lower energies than do monatomic ions.

Ions accelerated by high voltage possess relatively high kinetic energy; however, when they are injected into a material, they lose this energy through interactions with the material and eventually come to rest after traveling a certain distance. The energy lost during this process is described by the stopping power, which represents the energy loss per unit distance travelled by the ion. At low energies, ions primarily lose energy through elastic collisions with the atoms in the solid, a process quantified by the nuclear stopping power (S_n). As the ion energy increases, the ions not only collide with the atomic nuclei but also strongly interact with the electron system of the material, leading to additional energy loss. This component is described by the electronic stopping power (S_e). For example, when Xe ions are irradiated onto a Si target, S_n dominates over S_e at lower energies than ~2 MeV. However, as the ion energy increases, S_e becomes the dominant mechanism. At energies around 80 MeV, energy loss occurs primarily through interactions with electrons, and S_n becomes approximately two orders of magnitude smaller than S_e. Heavy ions in this high-energy regime, where the electronic stopping power far exceeds the nuclear stopping power, are referred to as swift heavy ions (SHIs).

The trajectory of SHIs is nearly linear, and cylindrical damage regions may form along this path—these are known as *ion tracks*. The tracks are often amorphous but can also exhibit damaged crystalline [1]. While the formation of such tracks depends on irradiation conditions (e.g., ion species, energy, and target material), the typical size of tracks created by monoatomic ions is approximately 10 nm or less in diameter and can extend several micrometers or more in length.

As aforementioned, the interaction between ions and solids in the high-energy regime, where track formation occurs, is primarily due to electronic excitation. Although tracks are damaged regions, their formation process differs from that of damage caused by low-energy ion irradiation wherein elastic collisions occur between incident ions and constituent atoms of the solid, resulting in damage. In contrast, high-energy ion irradiation initially excites the solid's electronic system, followed by energy transfer to the atomic system via electron–lattice interactions. Some of this energy remains as atomic disorder during the subsequent de-excitation and relaxation processes. In the 1990s, laser irradiation of semiconductors and insulators was extensively studied to induce atomic migration via electronic excitation [2], though the underlying electronic excitation mechanisms (self-trapped excitons) likely differ from those involved in SHI irradiation. The mechanism underlying track formation has been explored [3]; however, it remains unelucidated.

Ion tracks do not form in all materials [4]; for example, they are difficult to form in metals. While tracks have been observed in Ti [5], there have been no reports of track formation in noble metals. Even in semiconductors, high S_e values are typically required. Semiconductors with weak ionicity, such as Si, Ge, and GaAs [6], may require cluster ion irradiation [7–10], which can achieve higher S_e values, to enable track formation. In comparison, tracks are generally easier to form in insulators. However, an exception is diamond, where track formation has not been reported in prior research.

Many attempts to form tracks in diamond using monoatomic ion irradiation have been unsuccessful [11]. However, we successfully formed ion tracks in diamond using C_{60} ions with energies in the several MeV range [12]. Diamond has been shown to be a unique material in the context of track formation physics, and this finding may challenge the prevailing understanding of the underlying mechanisms. This review introduces the current state of research on track formation physics, presents the first report of ion track formation in diamond, and discusses its broader significance.

2. Ion track formation model and its significance in diamond

2.1 Ion track formation model

The inelastic thermal spike (i-TS) model is currently the most widely accepted framework for explaining ion track formation. In this model, the target solid is conceptually divided

into two subsystems: an electron system and a lattice system. The process begins with the ultrafast excitation of the electron system by energetic heavy ions (on the order of femtoseconds or less), followed by a slower energy transfer to the lattice system (up to several picoseconds). This non-equilibrium evolution is described by treating the electron and lattice systems as having different temperatures, that is, the electron temperature T_e and lattice temperature T_L. As shown in Eqs. (1) and (2), the time evolution of these temperatures is described using a pair of coupled thermal diffusion equations [3]:

$$C_e(T_e)\frac{\partial T_e}{\partial t} = \nabla\cdot(K_e(T_e)\nabla T_e) - g(T_e - T_L) + A \quad (1)$$

$$C_L(T_L)\frac{\partial T_L}{\partial t} = \nabla\cdot(K_L(T_L)\nabla T_L) + g(T_e - T_L) \quad (2)$$

Here, the subscripts e and L denote the electron and lattice systems, respectively. C, K, and T represent the specific heat, thermal conductivity, and temperature of each system. The first term on the right-hand side of each equation accounts for thermal diffusion within the system, while the second term represents the energy exchange between the electron and lattice systems. This exchange makes T_e and T_L equal. The coefficient g is the electron–lattice coupling constant, and A is a source term representing energy input from ion excitation, which affects only the electron system.

Equations (1) and (2) are used to calculate the time evolution of T_e and T_L. A region where the lattice temperature exceeds the melting or boiling point of the material (under atmospheric pressure) is interpreted as forming a track upon rapid cooling. Toulemonde et al [3]. extended this model by incorporating bold assumptions and numerically solving the heat diffusion equations to account for a wide range of experimental observations, making this version of the i-TS model the most widely adopted to date. However, the model has also been subject to much criticism. For example, the criterion for track formation is based on the lattice temperature exceeding the bulk melting point or boiling point of the material; however, the melting point and boiling point used in this case are those of the bulk material at atmospheric pressure. Nonetheless, ion tracks often have diameters of 10 nm or less, and the phase transition temperatures at such small scales are not necessarily equal to those of bulk materials. Furthermore, track formation involves transient melting or vaporization within a solid matrix. The surrounding solid exerts confinement, making volume expansion difficult and potentially inducing high pressures that may alter the melting or boiling points. Despite these complexities, such effects are generally not considered in the current formulation of the i-TS model.

2.2 Significance of track formation in diamond

As previously mentioned, the i-TS model is the most widely accepted mechanism for track formation. This model determines whether a track is formed based on whether the lattice temperature exceeds the melting point (or boiling point) of the target material. Diamond and graphite are allotropes—two different crystal structures composed solely of carbon atoms. Under low-pressure conditions, including ambient pressure, graphite is the stable phase, while diamond is metastable. For this reason, diamond does not "melt" upon heating, except under extremely high pressure [13]. Instead, heating diamond around the atmospheric pressure eventually causes it to transform into graphite, with further heating leading to sublimation [13,14]. This graphitization process is not a phase transition in the conventional sense, but a relaxation from a metastable to a stable phase. As such, it lacks a well-defined transition temperature. In typical thermal treatment using a conventional furnace, graphitization occurs at approximately 2000–2200 K, and sublimation at approximately 4200 K, over timescales of seconds to minutes [13,14]. In the context of the i-TS model, track formation is associated with thermal melting of the medium. Therefore, cases of track formation in diamond should be considered to have resulted from a mechanism other than thermal melting, necessitating a reconsideration of the existing model. While sublimation is consistent with the carbon phase diagram and represents a true phase transition, thermal calculations indicate that sublimation does not occur under the ion irradiation conditions examined in this study.

2.3 Track formation in diamond by C_{60} ion irradiation

Prior attempts seeking to form ion tracks in diamond by using monatomic ion irradiation have not been successful. In fact, the maximum energy deposition achievable in diamond using monatomic ions, irradiation with the heaviest U ions at several GeV, corresponding to the Bragg peak (see "Technical term"), has not resulted in track formation [11]. Attempts have also been made to create conditions that facilitate track formation by irradiating diamond using a property known as the *pre-damage effect*. The pre-damage effect refers to a property where damage applied to a material decreases its thermal conductivity, which in turn facilitates the trapping of heat. Furthermore, the electron–lattice interaction increases, resulting in a more efficient transfer of the excitation of the electronic system to the lattice system, thus making track formation easier than in an undamaged sample [6]. Prior research has examined cases wherein diamond was irradiated with neutrons to introduce defects, followed by irradiation with SHIs; however, track formation has not been observed [15]. Diamond microparticles were also irradiated with SHIs under the hypothesis that the microstructural conditions—resembling the pre-damage effect—might facilitate track formation [16]. However, although graphitization occurred, no tracks were observed.

We used C_{60} ions at several MeV to successfully form tracks in diamond [12]. C_{60} is a molecule (cluster) composed of 60 carbon atoms arranged in a shape similar to a soccer ball. This large molecule is ionized by gaining or losing one or two electrons, then accelerated and injected to a solid. As a result, the 60 carbon atoms are almost simultaneously implanted into a circular area approximately equal to the diameter of the C_{60} molecule (0.7 nm), inducing very strong electronic excitation. While the excitation caused by each carbon atom is not particularly large, their near-simultaneous implantation into such a small area yields a very high excitation *density*, one that far exceeds the excitation density produced by monatomic uranium ions at several GeV. Ion tracks were formed in diamond through irradiation with 2–9 MeV C_{60} ions.

However, although the high S_e value (electronic stopping power) of C_{60} ions at several MeV is certainly an important factor in track formation in diamond, uranium ions at several GeV can also produce similar S_e values. Therefore, the key factor governing track formation may instead lie in the so-

called *velocity effect* [17], wherein the energy transfer is confined to a narrower region in the case of C_{60} ions compared to GeV-range uranium ions—even if both have comparable S_e values.

2.4 Ion velocity effect

When a fast heavy ion passes through a solid, it collides with the solid's electrons, causing these electrons to be ejected at high speed. The high-energy electrons generated in this way are called δ-electrons. These δ-electrons are emitted on average in the radial direction from the ion's trajectory and transfer their energy to the surrounding material. The maximum energy $W_{\max}$ of the δ-electrons is given as follows [18]:

$$W_{\max} = \frac{4M_{\mathrm{ion}}m_{\mathrm{e}}}{(M_{\mathrm{ion}} + m_{\mathrm{e}})^2} E_{\mathrm{ion}} \approx 2m_{\mathrm{e}}v_{\mathrm{ion}}^2 \qquad (3)$$

which is proportional to the square of the velocity v_{ion} of the SHI. In other words, faster ions produce δ-electrons with higher energy (although there is some distribution), resulting in longer ranges. Considering a cylindrical volume around the ion's linear trajectory, δ-electrons with a longer range excite a larger volume. Even with the same S_{e} value (i.e., the same energy deposited per unit length), a faster ion excites a larger volume, leading to a lower excitation density. Meanwhile, heavier ions such as C_{60} ions move more slowly and produce δ-electrons with shorter ranges. This leads to a locally higher excitation density. This explains why track formation does not occur with GeV ions in diamond but does occur with C_{60} ions.

3. Ion track formation in diamond

3.1 Track formation and microstructure

The diamond samples used in this study were high-purity poly- and single-crystalline specimens prepared by CVD and purchased from Element Six Co. Figure 1 shows tracks formed in diamond by 9 MeV C_{60}^{2+} ion irradiation, observed in some different configurations. Figure 1(a) presents an observation from a direction perpendicular to the sample surface, where black, nearly circular dots were visible. These black dots appeared slightly distorted into ellipses oriented in the same direction, likely due to the ions being irradiated at a 7° angle from the surface normal of the sample. Figure 1(b) shows the same sample observed at a 30° tilt, where each black dot displayed a thin linear structure. In other words, the observed dots were not spherical but rather close to cylindrical in shape, consistent with the interpretation of ion tracks. Figures 1(c) and 1(d) show cross-sectional views of samples cut along the depth direction. A Pt film was deposited on the ion-irradiated surface prior to cutting to mark the surface position. The thick black layer corresponds to the Pt film, and many thin black lines extending from this layer toward the diamond are evident; these are considered to correspond to the dots seen in Figs. 1(a) and 1(b). Thus, the structure formed by ion irradiation is interpreted as cylindrical ion tracks with a high aspect ratio.

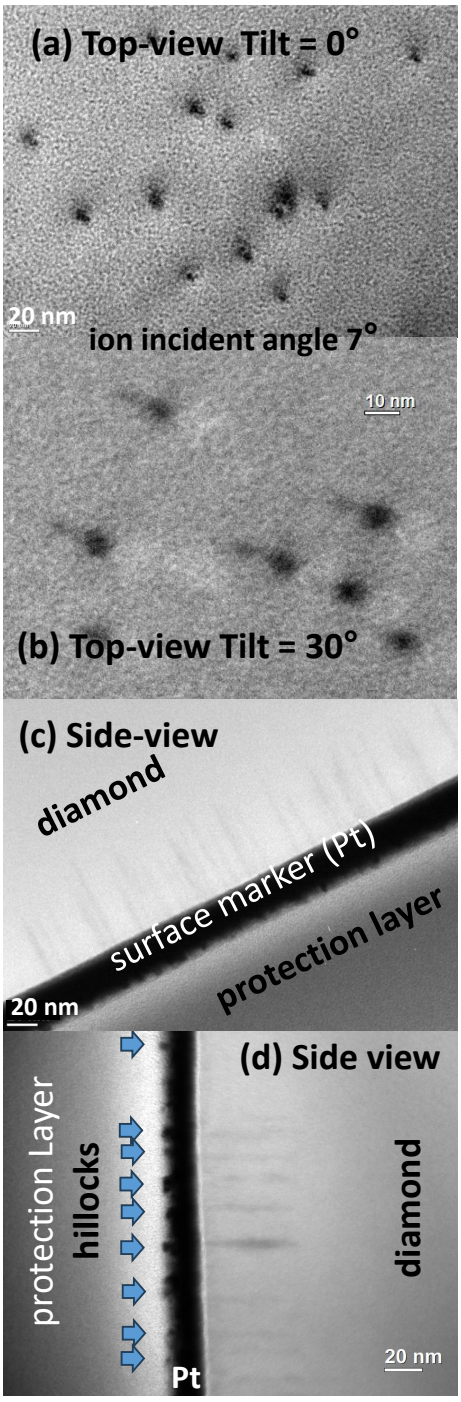

Fig. 1. Bright-field transmission electron microscopy (BF-TEM) images of diamond samples irradiated with 9 MeV C_{60}^{2+} ions [12]. Top-view images of irradiated diamond are shown with tilting angle of (a) 0° and (b) 30° from the surface normal. The C_{60} ion irradiations were performed to a fluence of 5×10^{10} C_{60}/cm^2 with an incident angle of 7° from the surface normal. Side-view images of ion tracks in (c) low- and (d) medium-magnifications. Thick black layers in (c) and (d) are deposited Pt films as surface marker. In (d), many protrusions are observed at the protection-layer side of the surface marker, which are probably due to the hillocks on the diamond surface. The fluence was 1×10^{11} C_{60}/cm^2 for (c) and (d).

Figure 1(d) shows the same arrangement as Fig. 1(c) but at a different location and slightly higher magnification; the focus must be on the protection layer side of the Pt layer and not the diamond side. Many protrusions approximately 5 nm in height were observed. The observed structures themselves appear to be composed of Pt; however, these protrusions were formed on the diamond surface, suggesting that the shapes observed in the Pt layer reflect the underlying surface morphology of the diamond. Pt protrusions were also observed extending along the tracks in the diamond layer, indicating that the protrusions on the diamond surface formed at the intersections of the tracks and the diamond surface. This phenomenon of surface protrusions forming at the intersection of tracks and the target material surface is well known as

hillock formation [19]. As aforementioned, tracks are considered to be generated in many materials as a result of a thermal melting transition. Pressure increases inside the track during melting, causing some molten material to escape at the intersection of the track and the surface, solidifying to form hillocks [19]. Although track formation in diamond is considered to occur via graphitization rather than thermal melting, the lower density of graphite compared to diamond may lead to increased pressure during graphitization. This pressure could displace the material toward the surface, producing protrusions.

Furthermore, the surface number density of the dot structures was counted to confirm whether the observed structures were tracks formed by C_{60} ion irradiation. The surface number density of the dot structures was approximately 5×10^{10} dots/cm^2, independent of the C_{60} energy. This value closely matched the C_{60} ion fluence of 5×10^{10}/cm^2. This agreement supports the interpretation that each dot structure corresponds to a single C_{60} ion impact on the diamond surface, confirming that the dot structures are tracks formed by C_{60} ion irradiation.

3.2 Dependence of track radius on electronic stopping power

Tracks were observed even in samples irradiated with 2 MeV; however, no structures resembling tracks could be confirmed in samples irradiated with 1 MeV. This suggests a threshold for track formation between 1 MeV and 2 MeV. Therefore, the average track radius R was calculated for each energy, and the square of this radius, R^2 (corresponding to the track's cross-sectional area), was plotted against the electronic stopping power S_e in Fig. 2. Although the data points were relatively scattered, they could be roughly fitted using the well-known empirical rule [6]:

$$R^2 = C(S_e - S_{e,th}) \tag{4}$$

where C is a proportionality constant and $S_{e,th}$ is the threshold of the electronic stopping power. The obtained $S_{e,th}$ was 24 keV/nm.

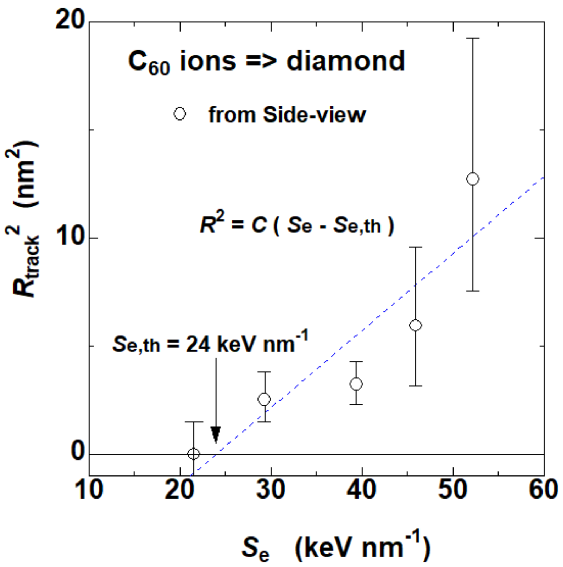

Fig. 2. Squared mean track radii determined from the side-view images are plotted against the electronic stopping power S_e [12]. Since the data points roughly fall on a straight line, the relationship of Eq. (4) is confirmed.

3.3 High-resolution TEM observation of tracks

Determining whether tracks formed in diamond were amorphous was of great interest and could be assessed by observing the lattice fringes within the tracks. However, carbon atoms have a small atomic number (six) and thus a small atomic radius. The lattice spacing of diamond crystals, composed of these small atoms, is also narrow, requiring high spatial resolution to observe lattice fringes. Figure 3 shows the results of observations using a high-resolution TEM with aberration correction. Figures 3(a), 3(b), and 3(d) show the same track at low, medium, and high magnifications, respectively. The images were obtained using scanning transmission electron microscopy bright-field mode (STEM-BF), rather than high-angle annular dark-field imaging (HAADF). More specifically, Fig. 3(d) was reconstructed using the spot within the red circle of the fast Fourier transform image shown in Fig. 3(c) to clarify the lattice fringes. Diamond lattice fringes were observed in many areas; however, the fringes were interrupted and appeared amorphous in the center of the track. The sample used for this observation was thinned to a thickness of 36 nm. The average track length at 9 MeV was 52.1 nm, with a standard deviation (SD) of 7.3 nm. As the sample thickness of 36 nm is 2 SD less than the average track length, the track almost certainly penetrated through the entire sample thickness.

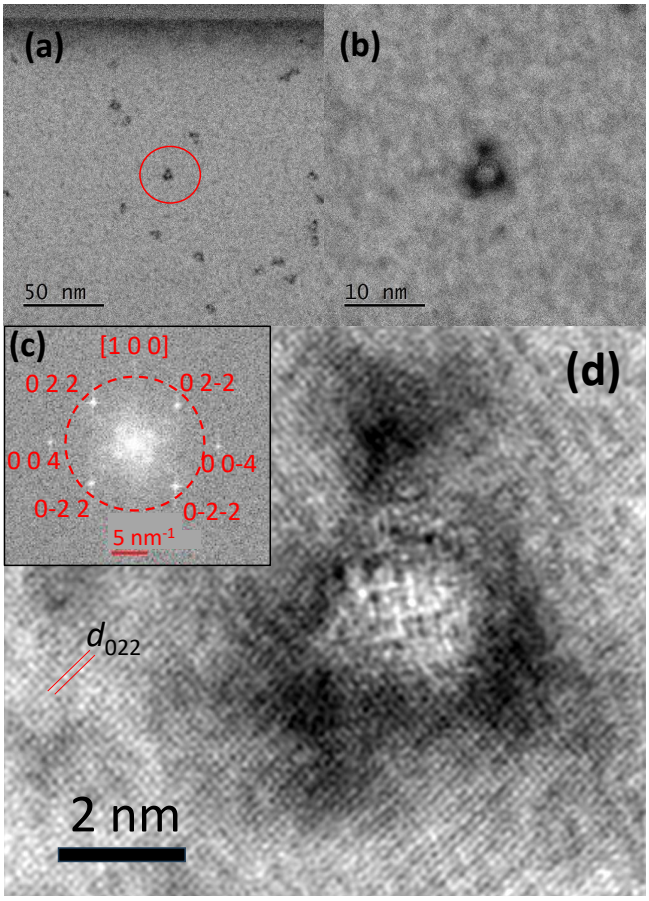

Fig. 3. Scanning transmission electron microscopy bright-field (STEM-BF) images of ion tracks formed under 9 MeV C_{60}^{2+} ion irradiation incident to the [100] zone axis of a single crystalline diamond. (a) low-, (b) medium-, and (d) high-magnification images of the same track. (c) a fast-Fourier transform (FFT) image of a high magnification image. (d) was reconstructed from the signal inside the red circle in (c).

3.4 Comparison with numerical simulations using two-temperature molecular dynamics

Section 2.1 introduces the i-TS model as a mechanism for ion track formation. This model separates the electron system and the lattice system and solves a pair of heat diffusion equations (Eqs. (1) and (2)), each described by the electron temperature and the lattice temperature. The region where the lattice temperature exceeds the melting point at atmospheric pressure is assumed to become a track. In recent years, the two-temperature molecular dynamics method (TT-MD) [20,21] has been proposed as an advancement beyond the i-TS model. The TT-MD method describes the electron system based on the electron temperature, as in conventional models, but computes the lattice system by using molecular dynamics (MD). The coupling between the electron and lattice systems randomly accelerates atoms in regions with high electronic temperature (with random acceleration directions). The method then examines atomic positions after sufficient time has passed and the structure has stabilized (approximately 100 ps after ion passage) to determine if damaged areas, such as tracks, have formed. An advantage of this approach is that it does not require assuming a phase transition temperature, such as the melting point of a solid. As aforedescribed, diamond is a metastable phase that does not melt but rather relaxes into the stable phase of graphite. This is not a phase transition but a relaxation to a stable phase; therefore, no clear transition temperature exists. In other words, the absence of a defined transition temperature prevents directly extending the phase transition framework of the i-TS model to graphitization. This work was conducted in collaboration with a group at the University of Helsinki, well known for their expertise in the TT-MD method.

Figure 4 shows the computational results. Figure 4(a) depicts the high ion velocity case (4.93 MeV/u, equivalent to a monatomic ion), while Fig. 4(b) shows the low ion velocity case (0.05 MeV/u, equivalent to a C_{60} ion). The results cover three S_e values, with atomic positions 100 ps after ion irradiation denoted by very small circles. The views are oriented along the [001] and [010] directions; thus, undamaged areas show only the atoms on the top surface, while atoms in the layers below overlap and remain hidden. This causes the undamaged areas to appear in light colors in the figures. Damaged areas have atoms displaced from their lattice positions, resulting in overlapping images that appear dark blue.

For the fast monatomic ion case (Fig. 4(a)), no tracks were observed at 20 keV/nm, while a track-like structure formed near the surface in the side view at 40 keV/nm, though it was broken and discontinuous. Tracks formed at 60 keV/nm; however, the maximum achievable S_e was 50 keV/nm even with uranium irradiation, making the attainment of such a high S_e impossible with monatomic ions. Figure 4(c) shows computed track diameters for fast monatomic ions with square marks. Corresponding experimental results are shown with purple marks, and there is generally good agreement. The slow C_{60} ion case (Fig. 4(b)) produced tracks even at 20 keV/nm, with track diameter increasing as S_e increased. Figure 4(c) shows computed track diameters with red circles and corresponding experimental results with green circles. The experimental and computed results show very good agreement, except at 20 keV/nm. It should be emphasized that no parameter adjustments were made to fit these results.

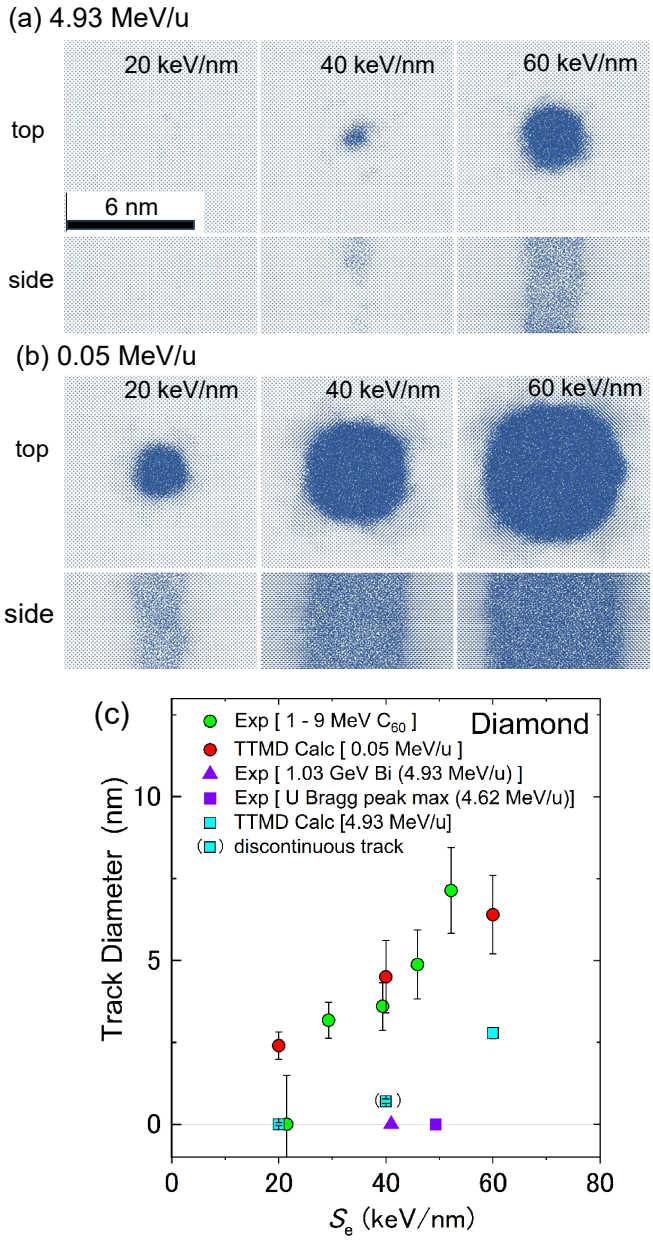

Fig. 4. Two-temperature molecular dynamics simulations of ion track formation in diamond [12]. Top- and side-views of simulation cells are shown for (a) high (4.93 MeV/u) and (b) low (0.05 MeV/u) velocity irradiations, at three different S_e = 20, 40, and 60 keV/nm. In (a) and (b), the locations of target atoms are shown by very small circles, after the simulations for 100 ps after the ion impact, which are viewed from [001] and [010], respectively. Since looking along the crystallographic axes, atoms are overlapped in undamaged regions except those in the uppermost layers, which results in weak color. Contrary, displaced atoms in damaged regions result in strong color. Experimentally and numerically determined track diameters were plotted in (c) against S_e. Green and red circles represent the experimental and simulated results for C_{60} irradiations. Purple symbols and cyan squares represent the experimental and simulated results for monatomic ion irradiation.

3.5 Remaining problem: incomplete graphitization of tracks

Electron energy loss spectroscopy (EELS) using scanning TEM is a technique that can reveal atomic bonding states at the nanometeric scale. Figure 5(a) shows the EELS spectrum of the carbon K absorption edge at a distance x, measured in one direction from the center of the track. The electron beam used for the measurement had a size of 0.5 nm. At the bottom

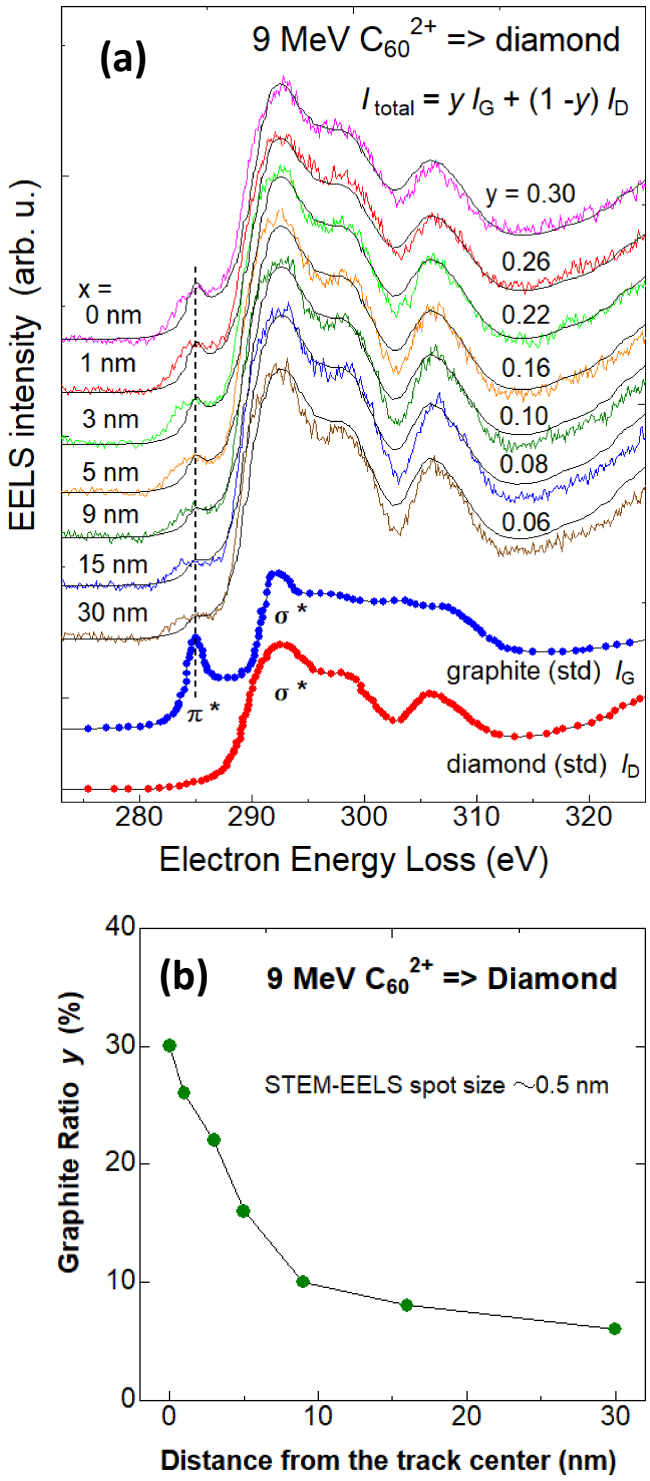

Fig. 5. Scanning transmission electron microscopy - electron energy loss spectroscopy (STEM-EELS) of an ion track in diamond [12]. The spectra at the carbon K-edge were detected with changing the distance x from the track center. The size of the electron beam was 0.5 nm in diameter. In the lower part of (a), standard spectra [22] of graphite and diamond are shown by blue and red circles. In the upper part of (a), experimental spectra are shown in thin colored curves. The black curves indicate the fitting results by Eq. (5). In (b), the graphite ratio y determined from the fitting is plotted along the distance from the track centers.

of Fig. 5(a), the standard spectra (reference values [22]) I_G and I_D for graphite and diamond are shown as blue and red circles, respectively. Graphite exhibits a sharp peak at 285 eV, corresponding to the transition from the 1s orbital to the antibonding π^* orbital. Meanwhile, diamond shows a valley structure at 303 eV, which is absent in graphite. The spectra (colored thin lines) observed in the irradiated sample exhibit both the π^* peak and the valley structure at every position x, indicating the coexistence of both components. Therefore, the measured spectrum at each position was fitted with a linear combination of the standard spectra I_G and I_D at a certain ratio y, as shown by Eq. (5).

$$I(E) = yI_G(E) + (1 - y)I_D(E) \quad (5)$$

which resulted in the fitted spectrum represented by the thin black line in the figure. Figure 5(b) shows the graphite ratio y plotted with respect to the distance x from the center of the track. Notably, the graphite ratio y was only approximately 30% even at the center of the track, with the diamond component remaining dominant. A positioning error was suspected as a possible reason, resulting in a location other than the track center being used as the reference point. However, 2D mapping also yielded nearly identical results. These findings suggest that the conventional understanding—that ion tracks in diamond are formed solely by graphitization and consist entirely of graphite—may need to be reconsidered.

4. Conclusion

Previous attempts to form ion tracks in diamond by using monoatomic ions have been unsuccessful. In this study, C_{60} ions were used to successfully form tracks at acceleration energies in the range of 2–9 MeV. However, this was not simply due to the extremely high S_e of C_{60} ions—an S_e value that cannot be achieved with monoatomic ions—as such extreme values were not necessarily used. As shown in Fig. 4(c), even with an equivalent S_e of 40 keV/nm, tracks were formed not via monoatomic ion irradiation but via C_{60} ion irradiation. In other words, track formation in diamond by C_{60} ions was not due to an extremely high S_e value but attributable to a velocity effect.

The high-resolution scanning TEM imaging showed that the center of the track became amorphous, and a surrounding structure was also observed. Although not shown in this paper, HAADF imaging revealed that a thicker region surrounded the thinner central region. This is likely the hillock observed as surface protrusions in the Pt layer in Fig. 1(d). Because graphite has a much lower density than diamond, the occurrence of graphitization within the track increases internal pressure, potentially causing material to be expelled from the center and deposited in the surrounding area.

It was previously assumed that diamond tracks were formed not by melting but via the thermal conversion from diamond to graphite by electronic excitation. However, as shown by the EELS results in Fig. 5, the graphite ratio was only approximately 30% even at the center of the track, indicating that 70% of the diamond remained. Further investigation is needed to clarify the mechanism of diamond track formation.

Acknowledgments

This research was supported by JSPS Grant-in-Aid for Scientific Research (KAKENHI) 22K04990 and 25K08531. This research was also conducted under the Inter-organizational Atomic Energy Research Program through an academic collaborative agreement among the Japan Atomic Energy Agency (JAEA), the National Institutes for Quantum Science

and Technology (QST), and the University of Tokyo. This research was also supported by the Ministry of Education, Culture, Sports, Science and Technology "Advanced Research Infrastructure for Materials and Nanotechnology in Japan (ARIM)" program (Project No. JPMXP1224NM5073).

References

[1] N. Ishikawa, T. Taguchi, and N. Okubo, J. At. Collis. Res. **18**, 43 (2021) [in Japanese].
[2] *Dynamics of Non-equilibrium Solid by Electronic Excitation –Towards the Creation of New Materials Science–*, ed. Y. Shinozuka and H. Katayama-Yoshida (Agne Gijutsu Center, Tokyo, 1993) [in Japanese].
[3] C. Dufour and M. Toulemonde, in *Ion Beam Modification of Solids*, ed. W. Wesch and E. Wendler, Vol. 61, p. 63 (Springer, 2016).
[4] M. Lang, F. Djurabekova, N. Medvedev, M. Toulemonde, and C. Trautmann, in *Comprehensive Nuclear Materials* (2nd Ed.), ed. R. J. M. Konings and R. E. Stoller, p. 485 (Elsevier, 2020).
[5] H. Dammak, A. Dunlop, D. Lesueur, A. Brunelle, S. Della-Negra, and Y. L. Beyec, Phys. Rev. Lett. **74**, 1135 (1995).
[6] A. Kamarou, W. Wesch, E. Wendler, A. Undisz, and M. Rettenmayr, Phys. Rev. B **78**, 054111 (2008).
[7] B. Canut, N. Bonardi, S. M. M. Ramos, and S. Della-Negra, Nucl. Instrum. Methods Phys. Res., Sect. B **146**, 296 (1998).
[8] A. Dunlop, G. Jaskierowicz, and S. Della-Negra, Nucl. Instrum. Methods Phys. Res., Sect. B **146**, 302 (1998).
[9] H. Amekura, K. Narumi, A. Chiba, Y. Hirano, K. Yamada, D. Tsuya, S. Yamamoto, N. Okubo, N. Ishikawa, and Y. Saitoh, Sci. Rep. **9**, 14980 (2019).
[10] H. Amekura, K. Narumi, A. Chiba, Y. Hirano, K. Yamada, S. Yamamoto, N. Ishikawa, N. Okubo, M. Toulemonde, and Y. Saitoh, Phys. Scr. **98**, 045701 (2023).
[11] M. Lang, U. A. Glasmacher, R. Neumann, D. Schardt, C. Trautmann, and G. A. Wagner, Appl. Phys. A **80**, 691 (2005).
[12] H. Amekura, A. Chettah, K. Narumi, A. Chiba, Y. Hirano, K. Yamada, S. Yamamoto, A. A. Leino, F. Djurabekova, K. Nordlund, N. Ishikawa, N. Okubo, and Y. Saitoh, Nat. Commun. **15**, 1786 (2024).
[13] I. Silvera, Nat. Phys. **6**, 9 (2010).
[14] R. A. Khmelnitsky and A. A. Gippius, Phase Transit. **87**, 175 (2014).
[15] R. A. Khmelnitski, V. V. Kononenko, J. H. O'Connell, V. A. Skuratov, G. F. Syrykh, A. A. Gippius, S. A. Gorbunov, and A. E. Volkov, Nucl. Instrum. Methods Phys. Res., Sect. B **460**, 47 (2019).
[16] F. Zhang, M. Lang, J. Zhang, and R. C. Ewing, Nucl. Instrum. Methods Phys. Res., Sect. B **286**, 262 (2012).
[17] A. Meftah, F. Brisard, J. M. Costantini, M. Hage-Ali, J. P. Stoquert, F. Studer, and M. Toulemonde, Phys. Rev. B **48**, 920 (1993).
[18] E. H. Lee, Nucl. Instrum. Methods Phys. Res., Sect. B **151**, 29 (1999).
[19] N. Ishikawa, N. Okubo, and T. Taguchi, Nanotechnology **26**, 355701 (2015).
[20] D. S. Ivanov and L. V. Zhigilei, Phys. Rev. B **68**, 064114 (2003).
[21] A. A. Leino, S. L. Daraszewicz, O. H. Pakarinen, K. Nordlund, and F. Djurabekova, EPL (Europhys. Lett.) **110**, 16004 (2015).
[22] D. Muller, https://muller.research.engineering.cornell.edu/spectra/graphite-and-diamond-c-k-edge-spectra/

Technical term

Bragg peak

Bragg peaks refer to both the peaks that appear in the energy dependence of the electronic stopping power and in the sample depth dependence of the stopping power. The term is used in the former sense in this study.

Profile

Hiroshi Amekura is currently a Chief Researcher in National Institute for Materials Science (NIMS), Japan, and has worked in NIMS since 1991. He received B.Sc. (1989) and M.Sc. (1991) from the University of Tokyo, and Ph.D. (1999) from Tsukuba University. In 1997 and 1998, he was a guest scientist in Forschungszentrum Juelich (FZJ), Germany. His current interests cover ion-solid interaction, fabrication and modification of nano-structures by ion beams, etc.